

Microinstability-based model for anomalous thermal confinement in tokamaks

To cite this article: W.M. Tang 1986 *Nucl. Fusion* **26** 1605

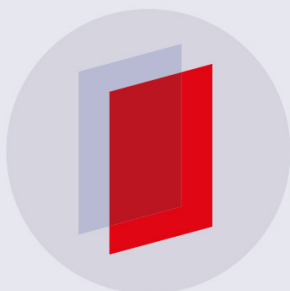
View the [article online](#) for updates and enhancements.

Related content

- [Transport simulations of Ohmic TFTR experiments with microinstability based, profile consistent models for electron and ion thermal transport](#)
M.H. Redi, W.M. Tang, P.C. Efthimion et al.
- [Anomalous thermal confinement in ohmically heated tokamaks](#)
F. Romanelli, W.M. Tang and R.B. White
- [Self-consistency of the principle of profile consistency results for sawtooth tokamak discharges](#)
V. Arunasalam, N.L. Bretz, P.C. Efthimion et al.

Recent citations

- [Investigation of key parameters for the development of reliable ITER baseline operation scenarios using CORSICA](#)
S.H. Kim *et al*
- [Survey of heating and current drive for K-DEMO](#)
D.R. Mikkelsen *et al*
- [Development of ITER non-activation phase operation scenarios](#)
S.H. Kim *et al*



IOP | ebooks™

Bringing you innovative digital publishing with leading voices to create your essential collection of books in STEM research.

Start exploring the collection - download the first chapter of every title for free.

MICROINSTABILITY-BASED MODEL FOR ANOMALOUS THERMAL CONFINEMENT IN TOKAMAKS

W.M. TANG
Plasma Physics Laboratory,
Princeton University,
Princeton, New Jersey,
United States of America

ABSTRACT. The paper deals with the formulation of microinstability-based thermal transport coefficients (χ_j) for the purpose of modelling anomalous energy confinement properties in tokamak plasmas. Attention is primarily focused on ohmically heated discharges and the associated anomalous electron thermal transport. An appropriate expression for χ_e is developed which is consistent with reasonable global constraints on the current and electron temperature profiles as well as with the key properties of the kinetic instabilities most likely to be present. Comparisons of confinement scaling trends predicted by this model with the empirical Ohmic database indicate quite favourable agreement. The subject of anomalous ion thermal transport and its implications for high density Ohmic discharges and for auxiliary heated plasmas is also treated.

1. INTRODUCTION

Experimental results from tokamak experiments have firmly established the fact that electron thermal transport is always anomalously large [1–3]. In addition, it has been observed (for instance in a number of neutral-beam-heated discharges) that the ion thermal confinement can also be significantly worse than the predictions of standard neoclassical theory [3]. The construction of transport models which can reproduce these trends is, of course, a difficult but vitally important task. Moreover, confidence in the predictive capability of such models basically requires that they be more physics based than empirical. In the present paper it is proposed that the physical processes primarily responsible for the anomalous thermal losses (during the ‘steady state’ phase of the discharges) are associated with low frequency microinstabilities. It is then demonstrated that a transport model based on their presence leads to results consistent with experimentally deduced confinement scaling trends.

Enhanced transport driven by drift type microinstabilities has long been a favoured candidate to account for the anomalous confinement properties observed in tokamaks [4, 5]. Comprehensive theoretical studies of threshold requirements have clearly indicated that these instabilities should be excited under realistic experimental conditions [6]. In addition, measurements using microwave and laser

scattering techniques have shown that the frequency and wavenumber spectra fall in the expected range and that the saturated amplitudes are consistent with mixing-length or ambient-gradient type non-linear estimates for these modes [4, 5]. On the other hand, just establishing the *presence* of such phenomena does not by itself prove that they are actually responsible for the anomalous transport observed. Supportive evidence to this effect requires the development of a microinstability-based transport model capable of reproducing the most significant trends in the confinement database.

Numerous theoretical transport models encompassing a wide variety of phenomena (both including and excluding drift type microinstabilities) have been proposed over the years. Because of the fundamental complexity of this non-linear problem, the models have invariably involved crucial assumptions (simplified geometry, expansion procedures, etc.) which have sparked continuous debates about relevance. It is therefore quite fortunate that in more recent years an increasingly extensive database (associated with steady state confinement properties) has been assembled [1, 2] which can be used to test the relevance of specific models. For example, statistical regression analysis of the data has yielded empirical scalings for energy confinement time, τ_E , and for electron temperature, T_e , with basic parameters such as toroidal field (B_T), total plasma current (I_p), etc. [1, 2, 7, 8]. In addition,

empirical forms for the electron thermal transport coefficient, $\chi_e(r)$, can be readily generated from data analysis codes [2] and compared with theoretically predicted behaviour.

With regard to earlier microinstability-based anomalous transport models [4, 5], a basic difficulty has been to formulate an expression for $\chi_e(r)$ which is applicable over most of the plasma radius. Since different physical effects (including those outside the realm of microinstability theories) are likely to be dominant in different regions of the plasma, it is not surprising that attempts at *globally* applying an expression for the electron thermal transport coefficient, which is based solely on local estimates of microinstability effects, have proven unsuccessful in reproducing experimentally deduced profiles for $\chi_e(r)$ and for the electron temperature, $T_e(r)$. Moreover, it should be recognized that any global prescription for $\chi_e(r)$ (valid during the steady state phase of tokamak discharges) must lead to temperature and current profiles compatible with macroscopic stability. Accordingly, in the present model, the microinstability-driven anomalous processes are constrained to maintain such profiles. The formulation of this 'profile-consistent' type constraint [9] is described in Section 2 and is used in Section 3 to construct a model for $\chi_e(r)$ which is applicable to ohmically heated discharges. Theoretically predicted anomalous electron thermal confinement properties are then compared with those from the Ohmic database. In Section 4 the subject of anomalous ion thermal transport is treated, and in Section 5 the basic conclusions and their implications for tokamak confinement are discussed.

2. PROFILE CONSTRAINT

The 'principle of profile consistency' [9] basically involves the empirical observation that dynamical processes in well-behaved tokamak discharges tend to maintain the same relative electron temperature profiles, $T_e(r)/T_{e0}$, and associated current profiles. These profiles are reasonably approximated by Gaussian shapes proportional to $\exp(-\alpha r^2/a^2)$ [9, 10]. The factor α appears to be primarily sensitive to the edge safety factor, $q_a \equiv aB_T/RB_p$, with a the plasma minor radius and R the major radius, and B_T and B_p the toroidal and poloidal magnetic field strengths. This trend has been observed in numerous Ohmic as well as neutral-beam-injected discharges with central heating deposition profiles [1, 8, 11]. In such cases,

$T_e(r)/T_{e0}$ is indeed found to be sensitive mainly to q_a irrespective of changes in density, plasma size, central temperature, and heating method. Further support for a profile-consistency constraint over confinement (steady state) time-scales is provided by results from pellet injection experiments on the Alcator C tokamak. Here it is observed that the readjustment of the electron temperature back to the usual Gaussian shape occurs about two orders of magnitude faster than τ_E [12].

Although no specific mechanisms have as yet been identified to enforce the observed global profiles, the allowed shapes are at least consistent with macroscopic stability requirements (i.e. long wavelength MHD instabilities). Moreover, such profiles do locally allow the presence of low frequency drift type microinstabilities [6]. In general, if the global radial dependence of the thermal transport coefficient is known, then knowledge of its magnitude in any local region of the plasma completely determines $\chi_e(r)$. Hence, the basic propositions here are: (i) the global radial dependence can be determined by assuming that a profile-consistency constraint is satisfied, and (ii) the local magnitude of $\chi_e(r)$ needed to complete the model can be determined by microinstabilities in the appropriate local region of the plasma.

In formulating the profile-consistency constraint, the starting point is the previously noted empirical observation that for central heating deposition profiles the experimentally measured electron temperature profiles are well approximated by

$$T_e(r) = T_{e0} \exp\left(\frac{-\alpha_T r^2}{a^2}\right) \quad (1)$$

with α_T primarily dependent on q_a [9–12]. Although this particular analytic form is convenient to use and represents a reasonable fit to the data, its choice here by no means suggests that other T_e -profiles (exhibiting a monotonically decreasing radial dependence sensitive primarily to q_a) could not be selected. Proceeding with Eq. (1), it can be used together with the parallel component of Ohm's law in steady state to determine the corresponding current profile, i.e. $E_{\parallel} = \eta_{\parallel}(r)J_{\parallel}(r)$ or

$$J_{\parallel}(r) = \sigma_{\parallel}(r)f_N(r)V/2\pi R \quad (2)$$

where $\eta_{\parallel}(r)$ is the effective parallel resistivity, $\sigma_{\parallel}(r)$ is the classical (Spitzer) conductivity, V is the loop

voltage, and $f_N(r)$ is the neoclassical conductivity reduction factor [13]. Noting that $\sigma_{||}(r) \propto [T_e(r)]^{3/2}/Z(r)$, with Z being the effective impurity concentration, Eqs (1) and (2) can be combined to give

$$J_{||}(r) = \bar{f}(r) J_{||0} \exp[-(3\alpha_T/2)(r^2/a^2)]$$

with $\bar{f}(r) \equiv f_N(r)Z_0/Z(r)$. Since the general expression for $f_N(r)$ appropriate for all collisionality regimes is a complicated function of r [13] and since the radial dependence of Z is very difficult to estimate (both theoretically and experimentally), the simplest choice is to take $\bar{f}(r) = 1$. Hence, the parallel current density for this approximate model becomes

$$J_{||}(r) = J_{||0} \exp(-\frac{\alpha_q r^2}{a^2}) \tag{3}$$

with $\alpha_q \equiv 3\alpha_T/2$.

In order to eliminate the arbitrary parameter, α_q , in terms of the physical parameter, q_a , first recall that the safety factor is given by

$$q(r) = (\frac{Bcr^2}{4\pi R}) / \int_0^r dr' r' J_{||}(r') \tag{4}$$

Combining this with Eq. (3) leads to the result

$$q(r) = \frac{q_a (r^2/a^2) [1 - \exp(-\alpha_q)]}{1 - \exp[-\alpha_q (r^2/a^2)]} \tag{5}$$

Numerous experimental measurements of the location of the $q = 1$ surface (deduced from the inversion position of the sawtooth signals) have indicated that the empirical formula

$$\frac{r_1}{a} = \frac{1}{q_a} \tag{6}$$

is a good approximation [1, 11]. This is illustrated in Fig. 1 with data points obtained from recent measurements taken on the TFTR tokamak for Ohmic as well as neutral-beam-heated discharges [11]. Using Eq. (6) in Eq. (5) then yields the result

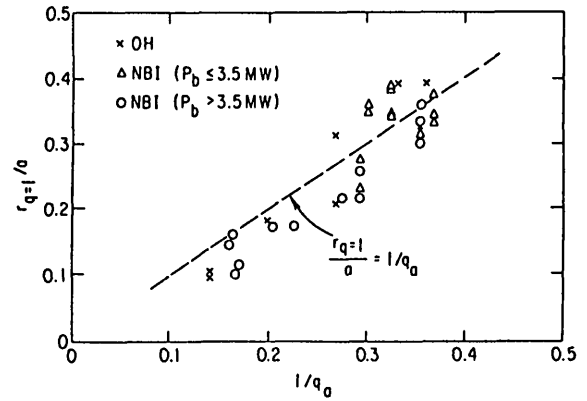


FIG. 1. Position of the $q = 1$ surface (r_1/a) obtained from measurements on the TFTR experiment [11] and plotted as a function of $1/q_a$.

$$\alpha_q = q_a + 0.5 \tag{7}$$

Hence, the resultant constrained profile shapes for $T_e(r)$, $J_{||}(r)$ and $q(r)$ in the present model do conform to the experimentally observed trend, i.e. the natural profile shapes are primarily a function of the edge safety factor, q_a [11].

3. ANOMALOUS ELECTRON THERMAL CONFINEMENT

In this section a microinstability-based model governing anomalous electron thermal transport properties in ohmically heated tokamak discharges is constructed. The starting point is the following simplified form of the steady state energy balance equation

$$E_{||} J_{||}(r) = -\frac{1}{r} \frac{d}{dr} [r n_e(r) \chi_e(r) \frac{d}{dr} T_e(r)] \tag{8}$$

in which Ohmic heating is equated to anomalous electron thermal losses. Since $E_{||} = V/2\pi R$ is approximately constant in radius, this can also be expressed in the form

$$\chi_e(r) = \frac{-E_{||} \int_0^r dr' r' J_{||}(r')}{r n_e(r) (d/dr) T_e(r)} \tag{9}$$

Application of the profile constraints described in Section 2 then gives $\chi_e(r) \equiv \chi_{eo}F(r)$, with

$$F(r) = \frac{\exp[(2/3)(q_a+0.5)(r/a)^2] - \exp[-(1/3)(q_a+0.5)(r/a)^2]}{(r/a)^2 [n_e(r)/n_o]} \quad (10)$$

and

$$\chi_{eo} \left(\frac{\text{cm}^2}{\text{s}}\right) = 4.6 \times 10^4 \left(\frac{a}{Rq_a}\right)^2 \frac{zB_T^2}{n_o T_{eo}^{5/2}} \quad (11)$$

where B_T (T), n_o (10^{14} cm^{-3}) and T_{eo} (keV).

In order to complete the model, it is necessary to determine the magnitude of T_{eo} (and thus that of χ_{eo}). As noted in Section 2, this can be accomplished by specifying the local magnitude of χ_e in any region of the plasma. In the present calculation, attention is directed to the 'good confinement zone' between the $q = 1$ and $q = 2$ surfaces. Experimentally, this region is usually observed to exhibit the most effective thermal insulation properties [14–16]; theoretically, it tends to be characterized by good magnetic surfaces [17] and by spatial gradients sufficiently large to drive drift type microinstabilities [15]. In addition, the collisionality parameter, $\nu_{*e} \equiv (\nu_{\text{eff}}/\omega_b)_e$ (with ν_{eff} and ω_b being thermal estimates, respectively, of the effective collision frequency and the bounce frequency of the trapped electrons [4]), is typically less than unity or of order unity in this local zone [5, 15]. With such considerations in mind, it is appropriate to propose that trapped-electron drift type microinstabilities are a likely cause of the anomalous transport in the region between the $q = 1$ and $q = 2$ surfaces.

At the simplest level, the local magnitude of the thermal transport coefficient can be approximated by the familiar estimate $\chi_e^\mu \cong \gamma/k_\perp^2$, with γ the characteristic growth rate and k_\perp the perpendicular wavenumber of the relevant microinstability. It should be remembered here that in estimates of this type, γ characterizes the strength of the instability and its use does not imply that the linear properties persist in the non-linear state [18]. Moreover, the fact that comprehensive numerical [6] as well as analytic [19] toroidal calculations have demonstrated that trapped-electron drift modes are strongly unstable in most parameter regimes of interest further motivates the use

of this strong turbulence type approximation.

Equivalent results can also be obtained by using f_e (the linearized perturbed distribution function) to calculate the anomalous thermal flux, Q_e , and then using the usual turbulence-based 'ambient-gradient' or 'mixing-length' estimate for the saturated amplitude of the perturbations [20, 21]. Accordingly, the local magnitude of χ_e due to trapped-electron effects can be approximated by

$$\chi_e^\mu = \frac{\epsilon^{3/2} (\omega_{*e}^2 \eta_e + \omega_{*e}^P \omega_{De})}{\nu_{ei} [1 + (\bar{C}/\nu_{*e})]} k_\perp^2 \quad (12)$$

where $\epsilon \equiv r/R$, $\eta_e = (L_n/L_T)_e$, with L_n and L_T the density and temperature gradient scale lengths, respectively, $\omega_{*e} = k_\perp c T_e / e B L_n$, $\omega_{*e}^P = \omega_{*e} (1 + \eta_e)$, $\omega_{De} = \omega_{*e} L_n / R$, and $\bar{C} \cong 0.1$ to 0.2 . Here the \bar{C} -term models the transition into the collisionless regime [20], and the ω_{De} -term represents the residual trapped-electron effects due to the presence of interchange-like ion instabilities occurring in the limit of very weak density gradients [22]. Neither of these modifications is usually appreciable in low to moderate density Ohmic discharges. Note also that since ν_{*e} represents the collisionality of the thermal particles, the higher energy trapped electrons can still contribute to γ even when the ν_{*e} exceeds unity [6, 19]. Hence, Eq. (12) can continue to be used in the lower collisionality end of the plateau regime.

Since Eq. (12) is indeed a rough approximation for the local magnitude of χ_e , it is appropriate to average it over its radial region of applicability. To do this, consider the associated entropy production [23]

$$S^\mu \equiv \chi_{eo}^\mu \int_{r_1}^{r_2} dr G(r) \left[\frac{d \ln T_e(r)}{dr} \right]^2 \quad (13)$$

where S^μ is the entropy produced between the $q = 1$ and $q = 2$ surfaces (designated by r_1 and r_2), with χ_{eo}^μ and $G(r)$ the magnitude and local radial dependence of χ_e^μ , respectively. In terms of these quantities, Eq. (12) gives

$$\chi_{eo}^\mu \left(\frac{\text{cm}^2}{\text{s}}\right) = 4.5 \times 10^4 C_\mu \left(\frac{a}{R}\right)^{1/2} \frac{T_{eo}^{7/2}}{R^2 B_T^2 n_{eo} Z} \quad (14)$$

where T_{eo} (keV), R (m), a (m), n_o (10^{14} cm $^{-3}$), B_T (T), C_μ is a scaling constant of order unity, and

$$G(r) = \left(\frac{r}{a}\right)^{3/2} \left[\frac{n_e(r)}{n_o}\right]^{-1} \left[\frac{T_e(r)}{T_{eo}}\right]^{7/2} \times \left[\frac{a}{L_n(r)} + \frac{a}{L_T(r)} + \frac{aR}{L_n(r)L_T(r)}\right] \quad (15)$$

In order to be consistent with the global prescription for $\chi_e(r)$ specified in Eqs (10) and (11), Eq. (13) is constrained to satisfy

$$S^H = S = \chi_{eo} \int_{r_1}^{r_2} dr r F(r) \left[\frac{d \ln T_e(r)}{dr}\right]^2 \quad (16)$$

Using Eqs (11) and (14) in Eq. (16) and solving for T_{eo} gives

$$T_{eo} \text{ (keV)} = B_T^{2/3} (RZ/q_a)^{1/3} (a/R)^{1/4} (\hat{C}/C_\mu)^{1/6} \quad (17)$$

with units as specified for Eq. (14), and

$$\hat{C} \equiv \frac{\int_{r_1}^{r_2} dr r F(r) \left[\frac{d \ln T_e(r)}{dr}\right]^2}{\int_{r_1}^{r_2} dr r G(r) \left[\frac{d \ln T_e(r)}{dr}\right]^2} \quad (18)$$

with $F(r)$ and $G(r)$ given by Eqs (10) and (15). Substituting this result back into Eq. (11) then gives for the magnitude of the thermal transport coefficient

$$\chi_{eo} \left(\frac{\text{cm}^2}{\text{s}}\right) = 4.6 \times 10^4 \frac{B_T^{1/3} a^{11/8} Z^{1/6}}{n_o R^{53/24} q_a^{7/6}} \left(\frac{C}{\hat{C}}\right)^{5/12} \quad (19)$$

The quantity \hat{C} in Eqs (17)–(19) can be readily calculated as a function of a/R and the parameters

characterizing the temperature and density profiles. As shown in Section 2, the appropriate choice for the temperature parameter is q_a , with the profile given by

$$T_e(r)/T_{eo} = \exp[-(2/3)(q_a+0.5)(r/a)^2]$$

With regard to the density, experimental measurements (e.g. Ref. [10]) indicate that the profiles are reasonably well represented by $n_e(r)/n_{eo} = [1 - (r/a)^2]^{\alpha_n}$, with the characteristic parameter α_n typically falling between 0.5 and 2. Using these forms, the integrals in Eq. (18) can be numerically evaluated as functions of q_a and α_n . The resultant parametric dependence is approximately given by

$$\hat{C}(a/R, q_a, \alpha_n) \approx 12 q_a (a/R)^{0.8} \alpha_n^{-0.5} \quad (20)$$

Using this in Eqs (17) and (19) then yields

$$T_{eo} \text{ (keV)} \approx 1.5 B_T^{0.7} a^{0.4} Z^{0.3} q_a^{-0.2} R^{-0.1} \alpha_n^{-0.1} C_\mu^{-0.2} \quad (21)$$

$$\chi_{eo} \left(\frac{\text{cm}^2}{\text{s}}\right) \approx 1.6 \times 10^4 C_\mu^{0.4} \alpha_n^{0.2} \frac{B_T^{0.3} a^{1.0} Z^{0.2}}{R^{1.9} q_a^{1.6}} \quad (22)$$

with $0.5 \leq \alpha_n \leq 2$ and C_μ being the order unity scaling constant from Eq. (14). Together with the radial dependence given by Eq. (10), Eq. (22) completes the prescription for a profile-consistent microinstability-based model for the anomalous electron thermal transport coefficient in low to moderate density ohmically heated tokamak plasmas.

In the discussion that follows, the anomalous electron thermal transport model just derived is applied to Ohmic scenarios of interest and the results are compared with the empirical database. Taking $\alpha_n = 1$ as being typical of density profiles in low to moderate density discharges and letting the scaling

constant, C_μ , be set to unity, Eqs (10) and (22) can be combined to give

$$\chi_e(r) \approx \frac{1.6 \times 10^4}{n_e(r)} \frac{a B_T^{0.3} Z^{0.2}}{R^{1.9} q_a^{1.6} (r/a)^2} \times \left\{ \exp\left[\frac{2}{3}(q_a + 0.5)\left(\frac{r}{a}\right)^2\right] - \exp\left[-\frac{1}{3}(q_a + 0.5)\left(\frac{r}{a}\right)^2\right] \right\} \quad (23)$$

with n_e (10^{14} cm^{-3}), B_T (T), R (m), a (m) and χ_e ($\text{cm}^2 \cdot \text{s}^{-1}$). Since there is strong experimental evidence that MHD sawtooth activity dominates effects inside the $q = 1$ surface ($r = r_1$), this model should be applied in the region between r_1 and the plasma edge.

As pointed out in Section 2, data analysis codes such as TRANSP [24] can be used to generate empirical forms for $\chi_e(r)$ which can be compared with theoretical models [2, 24]. Application of Eq. (23) to a representative set of Ohmic data from the PDX experiment [24] was found to yield reasonably good agreement with results from the TRANSP code empirical analysis of these cases.¹ In particular, the input parameters for the six shots studied were: $R = 1.43 \text{ m}$, $a = 0.42 \text{ m}$, $n_0 = 0.4 \times 10^{14} \text{ cm}^{-3}$, $Z = 3$, $B_T = 1.2\text{--}1.5 \text{ T}$, and $q_a = 2.1\text{--}3.6$. As shown by the typical case plotted in Fig. 2, the results for χ_e from the theoretical model correlate well with those obtained from the TRANSP code. Recent applications of this model to Ohmic data from the TFTR experiment have again led to similarly favourable comparisons with empirically generated values of $\chi_e(r)$ [26].

Theoretical estimates for the scaling properties of the central electron temperature, $T_e(0)$, and for the volume-averaged electron temperature, $\langle T_e \rangle$, can be readily obtained from Eqs (1) and (21). Since the rapid MHD sawtooth activity tends to flatten the temperature profile inside the $q = 1$ surface [8], the steady state central electron temperature is approximately given by $T_e(0) \cong T_e(r_1)$

¹ The results for the empirical values of $\chi_e(r)$ were obtained from applying the TRANSP code to a representative set of Ohmic PDX discharges by Kaye [25].

$\cong T_{e0} \exp[-(2/3)(q_a + 0.5)/q_a^2]$. Again taking both C_μ and α_n equal to one, Eq. (21) leads to the following scaling for the central electron temperature

$$T_e(0) \propto B_T^{0.7} q_a^{0.2} a^{0.4} R^{-0.1} Z^{0.3} \quad (24)$$

Since $q_a \propto a^2 B_T / I_p R$, an equivalent form is given by

$$T_e(0) \propto B_T^{0.9} Z^{0.3} a^{0.8} R^{-0.3} I_p^{-0.2} \quad (25)$$

The trend predicted here can be compared with experimentally measured values obtained from the PLT and TFTR tokamaks. Statistical regression analysis of the database yields the empirical scaling [8]

$$T_e(0) \text{ (DATA)} \propto B_T^{0.8} Z^{0.5} a^{1.0} R^{0.3} I_p^{-0.2} \quad (26)$$

which is in good agreement with the theoretical scaling specified by Eq. (25). The actual data points used in these studies are plotted as a function of Eq. (26) in Fig. 3.

With regard to the volume-averaged electron temperature, the theoretical model yields the scaling

$$\langle T_e \rangle \propto B_T^{0.7} q_a^{-0.7} a^{0.4} R^{-0.1} Z^{0.3} \quad (27)$$

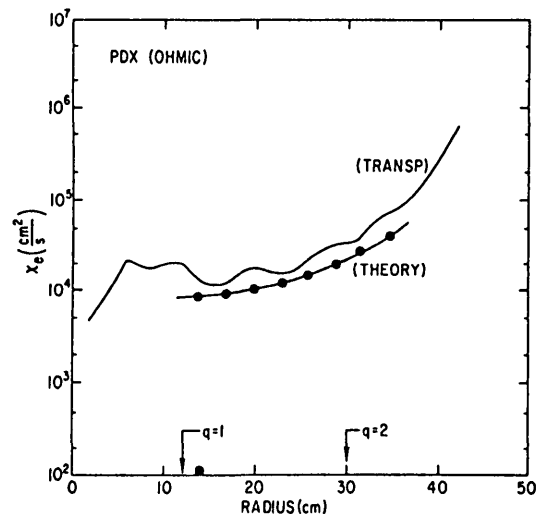


FIG. 2. Comparison of $\chi_e(r)$ obtained from the theoretical model, Eq. (23), and from the TRANSP code empirical analysis. This is a representative Ohmic PDX case with $R = 1.43 \text{ m}$, $a = 0.42 \text{ m}$, $Z = 3$, $n_0 = 0.4 \times 10^{14} \text{ cm}^{-3}$, $B_T = 1.5 \text{ T}$ and $q_a = 3.6$.

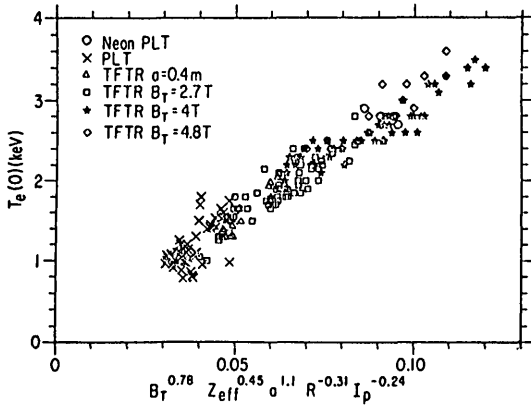


FIG. 3. Experimentally measured central electron temperature plotted against the empirical scaling obtained from a regression analysis of TFTR and PLT data [8].

This result can be compared with the empirical scaling obtained from a regression analysis of the large Ohmic database assembled in Ref. [27], i.e.

$$\langle T_e \rangle \text{ (DATA)} \approx B_T^{0.9} q_a^{-0.9} a^{0.5} R^{-0.2} Z^{0.5} n_o^{-0.1} \quad (28)$$

Here again the correlation is quite favourable. Note also that combining Eqs (24) and (27) yields

$$\langle T_e \rangle / T_e(0) \approx q_a^{-0.9} \quad (29)$$

As illustrated by Fig. 4, this result is in good agreement with recent trends observed in the TFTR experiment [11].

The electron energy confinement time, $\tau_{E,e}$, can be estimated by

$$\tau_{E,e} = \frac{(3/2) \int_0^a dr r n_o(r) T_e(r)}{\int_0^a dr r \eta_{||}(r) J_{||}(r)} \quad (30)$$

Using the profile model of Section 2 together with Eq. (8) then gives

$$\tau_{E,e} \approx a^2 I(\alpha_n, q_a) / (q_a + 0.5) \chi_{e0} \quad (31)$$

with

$$I(\alpha_n, q_a) = \int_0^1 dx x (1 - x^2)^{\alpha_n}$$

$$\times \exp\left[-\frac{2}{3} (q_a + 0.5)x^2\right] \quad (32)$$

For low to moderate density Ohmic discharges, Eq. (23) can be substituted into Eq. (31) to yield (with $\alpha_n = 1$)

$$\tau_{E,e} \text{ (s)} \approx 0.1 n_o R^{1.9} a^{1.0} q_a^{0.5} B_T^{-0.3} Z^{-0.2} \quad (33)$$

Since experimental evidence indicates that the electron loss channel tends to be dominant in this density regime [1, 24], the total energy confinement time, τ_E , should scale with $\tau_{E,e}$. This result can therefore be compared with the empirical scaling deduced from the large Ohmic database analysed in Ref. [1], i.e.

$$\tau_E \text{ (DATA)} \approx n_o R^{2.0} a^{1.0} q_a^{0.5} \quad (34)$$

Hence, the theoretical scaling given in Eq. (33) is in reasonable agreement with the ‘Neo-Alcator empirical scaling’ which, in turn, is consistent with recent confinement scaling trends observed in ohmically heated TFTR discharges [28]. The associated data are displayed in Fig. 5.

Since the electron temperature is a dependent variable, it was expressed in terms of ‘design’ variables, such as B_T and a , in the final expression for $\chi_e(r)$ given in Eq. (23). Nevertheless, if so desired, the transport coefficient can also be expressed in terms of the temperature. Specifically, if Eq. (21) is used to eliminate B_T in terms of T_{e0} , Eq. (23) becomes

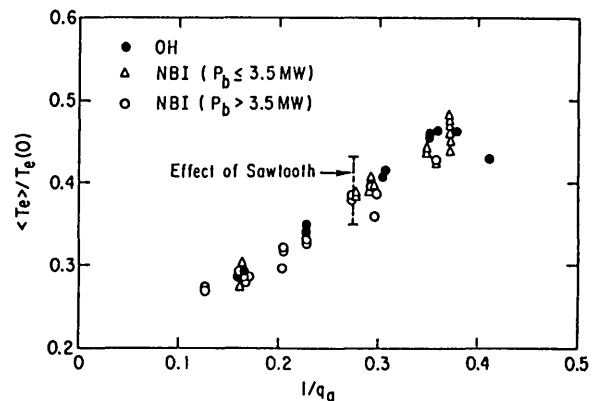


FIG. 4. Experimentally measured ratio of volume-averaged to central electron temperature plotted as a function of $1/q_a$.

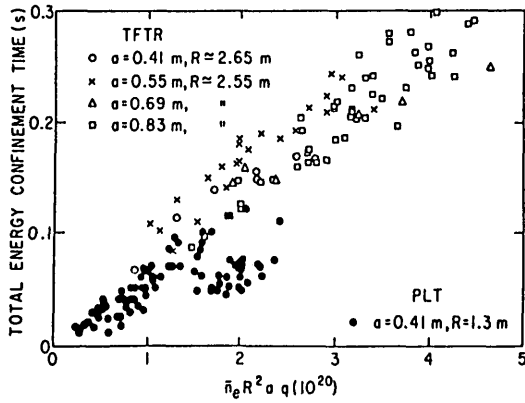


FIG. 5. Total energy confinement time plotted against $\bar{n}_e R^2 a q$ for Ohmic data from the TFTR and PLT experiments.

$$\chi_e(r) = \frac{1.3 \times 10^4}{n_o} \frac{a^{0.8} T_{eo}^{0.5}}{R^{1.8} q_a^{1.5}} F(r) \quad (35)$$

with $F(r)$ defined by Eq. (10) and T_{eo} in keV. Notice that although this exhibits an unfavourable scaling with temperature, it is not nearly as dramatic as the $T_{eo}^{7/2}$ dependence often cited as being characteristic of microinstability-based transport models. However, as indicated by the local microinstability-based expression for χ_e given in Eq. (14), the actual dependence is $T_{eo}^{7/2}/B_T^2$. Since T_{eo} is a function of B_T via Eq. (21), the resultant scaling of χ_e with either variable is relatively weak.

It is interesting to note that the anomalous electron thermal transport coefficient can also be expressed in terms of the Ohmic power, P_{OH} , with

$$P_{OH} \equiv 4\pi^2 R \int_0^a dr r \eta_{||}(r) J_{||}(r)$$

As in the case of T_{eo} , this quantity is also a dependent variable. Nevertheless, repeating the procedures described in Sections 2 and 3, but treating P_{OH} as a distinct variable, leads to the result

$$\chi_e(r) = \frac{7.7 \times 10^3}{n_o} \frac{P_{OH}^{0.8} F(r)}{R^{1.2} q_a^{0.9} B_T^{0.4} Z^{0.2} a^{0.1}} \quad (36)$$

with $F(r)$ given by Eq. (10) and P_{OH} in MW. The corresponding Ohmic confinement time scaling can be expressed as

$$\tau_{E,e} \propto P_{OH}^{-0.8} n_o B_T^{0.4} R^{1.1} a^{2.1} Z^{0.2} \quad (37)$$

This degradation of confinement with increasing power is analogous to the usual trend observed in auxiliary heated tokamak discharges [1, 2].

As a final point in this section, it should be noted that Eqs (23), (35) and (36) are, of course, entirely equivalent forms. In particular, when applied to actual transport codes, it has been demonstrated that (as expected) they give the same results [29]. The usefulness of Eqs (35) and (36) lies in the fact that they clearly indicate that there should be an unfavourable scaling of anomalous electron transport with temperature and with input power in ohmically heated discharges.

4. ANOMALOUS ION THERMAL CONFINEMENT

From a microinstability-based perspective it can be argued that there should *always* be some level of anomalous enhancement of ion thermal transport. The basic reason for this is that once instabilities are excited, the resultant electric fields will act on *both* species. This should be true regardless of whether the actual destabilizing mechanisms are dominated by ions or by electrons. However, it should also be remembered that unlike the particle transport situation (and its associated ambipolar constraint), the microinstability-driven electron thermal transport can be different from the corresponding ion transport. This will be further explained in the following discussions.

In the preceding section it was demonstrated that trapped-electron drift type instabilities could be primarily responsible for the observed anomalous transport. It was pointed out there that the associated local thermal diffusivity (in the 'good confinement' zone) effectively determines the magnitude of χ_e . In fact, simple zero-dimensional arguments, based on local estimates for χ_e such as Eq. (12), together with the assumption that thermal confinement exists only within the $q = 2$ surface, have previously been used to obtain scaling predictions for τ_E and for $T_e(0)$ [30, 31], in reasonable agreement with empirical trends. Of course, a proper representation of the plasma properties across the discharge requires the application of realistic profile constraints such as the prescription given in Section 2. Hence, in estimating the magnitude of χ_i , the local analysis

used to obtain χ_e (i.e. Eq. (12)) can again be applied. Specifically, the anomalous ion thermal flux, Q_i , can be calculated using f_i (the linearized perturbed ion distribution function) together with the same amplitude estimate for the saturated potential fluctuations as that used to determine Q_e . In other words, this is just the response of the ions to the electric fields excited by the electron dynamics. Applying the usual formalism [20, 21], it is found that the local ion thermal diffusivity, χ_i^μ , is typically smaller than χ_e^μ and has a similar scaling, i.e. $\chi_i^\mu \cong \alpha_i \chi_e^\mu$, with χ_e^μ given by Eq. (12). The numerical factor, α_i , ranges from about 0.5 to 1, with the larger values falling in the collisionless regime. This trend is maintained, provided the gradient parameter, $\eta_i \equiv d \ln T_i / d \ln n_0$, remains below the threshold, $(\eta_i)_c$, for the onset of toroidal ion temperature gradient modes [32].

In order to assess the possible significance of anomalous ion effects in Ohmic discharges, a simplified pair of steady state energy balance equations is considered, i.e.

$$P_\Omega - P_{ei} = - \frac{1}{r} \frac{d}{dr} \left(r n_e \chi_e \frac{dT_e}{dr} \right) \quad (38)$$

$$P_{ei} = - \frac{1}{r} \frac{d}{dr} \left(r n_i \chi_i \frac{dT_i}{dr} \right) \quad (39)$$

where P_Ω is the Ohmic heating power used in Eq. (8) and P_{ei} is the electron-ion collisional power transfer term [23]. For low to moderate density regimes, P_{ei} is usually small, so that Eq. (8) remains a reasonable model for energy balance. Moreover, even if corrections to P_{ei} due to anomalous effects [33] were important, the structure of the total energy balance equation would remain approximately the same as Eq. (8) since, as just noted, χ_i^μ scales as χ_e^μ in this regime of collisionality. However, at high densities, the ion loss channel can become dominant since P_{ei} scales with the square of the density and since $\chi_e \propto 1/n_0$. If $\eta_i < (\eta_i)_c$, then the anomalous ion diffusivity (which scales as χ_e) will accordingly be smaller than the conventional neoclassical ion transport, χ_i^{NEO} , in this regime. This is an example of a situation where anomalous ion effects, though present, are masked by the magnitude of the ion neoclassical thermal losses, $[\chi_i^{\text{NEO}} \cong (m_i/m_e)^{1/2} \chi_e^{\text{NEO}}]$, thereby leading to the familiar conclusion that the electron channel is anomalous while the ions are neoclassical.

Previous calculations [34, 35] have shown that the observed saturation of τ_E at high densities in Ohmic discharges is consistent with the neoclassical picture. The experimental conditions studied involved density profiles similar to the usual shapes found in lower density regimes. However, in more recent experiments involving refuelling by gas puffing, the measured density profiles were found to be flatter and the energy confinement time saturation was observed to occur at considerably lower values than predicted by neoclassical theory [36, 37]. Under these circumstances it is quite likely (despite the absence of direct T_i -profile measurements) that η_i has exceeded $(\eta_i)_c$, i.e. $\eta_i \geq 1$ to 2. Hence, the toroidal η_i -modes (associated with sufficiently large values of η_i and unfavourable magnetic curvature effects) could be responsible for the τ_E -saturation below the neoclassical limit. This microinstability-based explanation was first posed in Ref. [38] and systematically investigated in recent studies involving time dependent [39] and steady state [40] transport codes. Results from these studies have indeed been found to be consistent with the observed trends. Specifically, for the flatter density profiles (large η_i), density saturation occurs well below the neoclassical limit, and for more peaked density profiles (smaller η_i), density saturation moves closer to the neoclassical prediction [39, 40].

In addition to the high density Ohmic cases just discussed, evidence for anomalous ion thermal transport has also been found in tokamaks heated by neutral beam injection (NBI) [2, 3]. Experimental results have indicated that if $\chi_i = C_{\text{NEO}} \chi_i^{\text{NEO}}$ is used in data analysis codes, then reproducing the value of the central ion temperature, $T_i(0)$, usually requires a numerical factor greater than unity for C_{NEO} . This rather unsatisfactory means of data analysis in the ion channel is necessitated by the fact that, until recently [3], the ion temperature profiles have usually not been measured. Nevertheless, the size of the neoclassical multiplier, C_{NEO} , in such studies at least provides indirect evidence for possible anomalous enhancement of ion thermal losses. Far more compelling direct support has come from very recent charge-exchange ion temperature profile measurements on NBI-heated Doublet III discharges [3]. Results indicate that the ion thermal diffusivity, $\chi_i(r)$, is not only larger than χ_i^{NEO} but also exhibits a dramatically different profile. In particular, $\chi_i(r)$ is found to rise towards the edge of the plasma and is roughly equal in both magnitude and shape to the experimentally deduced electron thermal diffusivity, $\chi_e(r)$ [3]. Since the ion temperature profiles in these discharges can be

sufficiently peaked to drive η_i -type modes, the proposition here is that the associated transport could account for the observed behaviour in the ion channel.

Comprehensive linear studies have indicated that if $\eta_i > (\eta_i)_c$, the resultant tokamak microinstabilities are dominated by ion dynamics rather than electron dynamics [22]. These toroidal η_i -driven modes are fluid like in character and (unlike the electron drift modes) tend to be insensitive to collisions. The local ion thermal diffusivity, which can be estimated by the methods noted earlier, is approximately given by

$$\chi_i^\mu \approx (\omega_{*i}^T \omega_{Di} T_e / T_i)^{1/2} / k_i^2 \quad (40)$$

with $\omega_{*i}^T = k_i c T_i / |e| B L_{Ti}$ and $\omega_{Di} = \omega_{*i}^T L_{Ti} / R$.

In terms of the magnitude and local radial dependence, this becomes $\chi_i^\mu(r) = \chi_{io}^\mu H(r)$, where

$$\chi_{io}^\mu \approx 1.2 \times 10^5 C_\eta \frac{T_{io}^{3/2}}{B^2 (Ra\tau)^{1/2}} \quad (41)$$

$$H(r) = \left(\frac{T_i(r)}{T_{io}} \right)^{3/2} \left(\frac{a}{L_{Ti}(r)} \right)^{1/2} \quad (42)$$

C_η is a scaling constant of order unity, $\tau \equiv T_e / T_i$, and the units are as given for Eq. (14). If trapped-ion effects (e.g. 'trapped-ion modes' with large η_i [41]) are taken into account, modifications to Eq. (40) are found to be relatively minor and will not be further considered here.

The anomalous electron thermal diffusivity associated with the η_i -modes can also be estimated by the methods noted earlier (i.e. using the saturated potential for these instabilities in evaluating Q_e). Because of the strong dependence of f_e on the effective electron collision frequency, the resultant χ_e tends to be smaller than χ_i and has a scaling similar to Eq. (12). However, in the more collisionless regime ($\nu_{*e} \ll 1$, appropriate to many NBI heated discharges [2, 3, 30]), the thermal diffusivities here (as in the case of collisionless electron drift modes) are roughly equal, i.e. $\chi_e \approx \chi_i$.

For auxiliary heated discharges the simplest form of the total energy balance equation in steady state is given by

$$P_H(r) = -\frac{1}{r} \frac{d}{dr} \left[r (n_e \chi_e \frac{dT_e}{dr} + n_i \chi_i \frac{dT_i}{dr}) \right] \quad (43)$$

with P_H being the total (Ohmic plus auxiliary) heating power. This equation can be easily solved, provided (i) the density and temperature profiles for the ions are approximately the same as those for the electrons, and (ii) the plasma is sufficiently collisionless, i.e. $\nu_{*e} \lesssim 0.1$ to 0.2 . As just noted, the second condition leads to χ_e and χ_i being similar in magnitude and scaling, so that, together with the first condition, the profile-consistent constraint of Section 2 can again be applied. Equation (43) then reduces to

$$\chi_e(r) \approx \chi_i(r) \approx \frac{-\bar{P} \int_0^r dr' r' h(r')}{(1+\tau) r n(r) \frac{d}{dr} T_i(r)} \quad (44)$$

where $P_H(r) \equiv \bar{P} h(r)$, with \bar{P} being the power per unit volume, and $h(r)$ being the deposition profile. Defining $\chi_i(r) \equiv \chi_{io} F_H(r)$ and applying the profile model of Section 2 yields

$$F_H(r) = \frac{\exp[2/3(q_a + 0.5)(r/a)^2]}{(r/a)^2 n(r)/n_o} \times \frac{\int_0^{r/a} dx' x' h(x')}{\int_0^1 dx' x' h(x')} \quad (45)$$

$$\chi_{io} \left(\frac{\text{cm}^2}{\text{s}} \right) \approx 1.2 \times 10^4 \frac{P_T}{n_o R T_{io} (1+\tau) \alpha_q} \quad (46)$$

where P_T is the total power in megawatts, n_o (10^{14} cm^{-3}), R (m), T_{io} (keV) and $\alpha_q = q_a + 0.5$.

As in the derivation of the profile-consistent form of $\chi_e(r)$ for Ohmic discharges, it is necessary to determine the magnitude of T_{io} (and hence χ_{io}). Using Eqs (41) and (42) to specify the local magnitude of χ_i and following the procedures leading to Eq. (17) of Section 3 then yields

$$T_{io} \text{ (keV)} \approx 0.4 B_T^{0.8} \left(\frac{P_T}{n_o} \right)^{0.4} \left(\frac{a}{R} \right)^{0.2} \left(\frac{\hat{C}_i}{C_\eta} \right)^{0.4} \times (\alpha_q)^{-0.6} (\tau)^{0.2} (1+\tau)^{-0.4} \quad (47)$$

where

$$\hat{C}_i \equiv \frac{\int_{r_1}^R dr r F_H(r) [d \ln T_i(r)/dr]^2}{\int_{r_1}^R dr r H(r) [d \ln T_i(r)/dr]^2} \quad (48)$$

with $H(r)$ and $F_H(r)$ specified by Eqs (42) and (45), and $d \ln T_i(r)/dr = (-4\alpha_q/3)(r/a^2)$. Substituting this result back into Eq. (46) gives for the magnitude of the thermal transport coefficient

$$\chi_{i0} \left(\frac{\text{cm}^2}{\text{s}} \right) = 3.0 \times 10^4 \left(\frac{P_T}{n_0} \right)^{0.6} (B_T R)^{-0.8} (a)^{-0.2} \\ \times (\alpha_q)^{-0.4} \left(\frac{C}{\tau} \right)^{0.4} (\tau)^{-0.2} (1+\tau)^{-0.6} \quad (49)$$

where C_η is the order unity scaling constant from Eq. (41), and \hat{C}_i as defined by Eq. (48) needs to be numerically evaluated as a function of q_a , α_n (the density profile parameter), and $h(r)$, the heating deposition profile of Eq. (44). Hence, the proposed model for the anomalous ion thermal transport coefficient in auxiliary heated discharges (where $\eta_i > (\eta_i)_c$) has the form

$$\chi_i(r) = \chi_{i0} F_H(r) \quad (50)$$

with χ_{i0} given by Eq. (49) and $F_H(r)$ specified by Eq. (45). In a sufficiently collisionless plasma (see, for instance, Ref. [3]) the corresponding electron thermal diffusivity is approximately the same, i.e. $\chi_e(r) \cong \chi_i(r)$. As noted earlier, at higher collisionality the response of the electron channel to the presence of η_i -modes exhibits a scaling for χ_e similar to that associated with the usual dissipative trapped-electron modes. Accordingly, in this regime, Eq. (36) can be applied, with P_T replacing P_{OH} and with $F_H(r)$ (given by Eq. (45)) replacing $F(r)$.

Since the heating profile in many NBI discharges tends to be more peaked (compared, for example, with Ohmic cases), the primary parametric dependence in Eq. (48) can be analytically estimated to give $\hat{C}_i \propto \alpha_q^{5/4}$. Using this approximation in Eq. (50) then leads to

$$\chi_i(r) \approx C_H \\ \times 10^4 \frac{P_T^{0.6} n_0^{0.4} \exp[(2/3)(q_a + 0.5)(r/a)^2]}{(RB_T q_a)^{0.8} a^{0.2} n(r)(r/a)^2} \quad (51)$$

where $C_H[\alpha_n, h(r), \tau]$, as a rough estimate, is taken simply to be a scaling constant. The corresponding scalings for the central ion temperature, $T_i(0) \cong T_i(r_1) \cong T_{i0} \exp[-(2/3)(q_a + 0.5)/q_a^2]$, and for the confinement time, $\tau_E \propto \tau_{E,i}$, become, respectively,

$$T_i(0) \propto \left(\frac{P_T}{n_0} \right)^{0.4} (B_T)^{0.8} \left(\frac{a}{R} \right)^{0.2} (q_a)^{0.3} \quad (52)$$

$$\tau_E \propto \left(\frac{n_0}{P_T} \right)^{0.6} R^{1.8} I_p^{1.0} a^{0.2} B_T^{-0.2} \quad (53)$$

The scalings in Eqs (52) and (53) are similar to the trends for the central electron temperature, $T_e(0)$, and for τ_E predicted in previous theoretical studies of NBI heated discharges [30]. However, in the earlier work, which assumed that only the electron channel is anomalous, the results came from zero-dimensional arguments based on local estimates for the electron thermal diffusivity associated with collisionless trapped-electron drift modes. In contrast, the toroidal ion temperature gradient modes, which are insensitive to collisions, are proposed in the present paper as the primary cause of enhanced transport in both the ion and electron channels. The similarity in the scalings derived from these different models in the low collisionality regime results because the local thermal diffusivity for the collisionless electron drift modes is very similar to Eq. (41) for the ion drift modes. Recent time-dependent transport code simulations have also invoked the presence of η_i -type instabilities to successfully model the behaviour of a number of NBI heated Doublet-III discharges [41].

Finally, the theoretically predicted trends in Eqs (52) and (53) can be compared with those deduced from the L-mode database for NBI heated tokamaks [1, 2]. As emphasized in Ref. [30], the experimental results correlate very well with the theoretical prediction

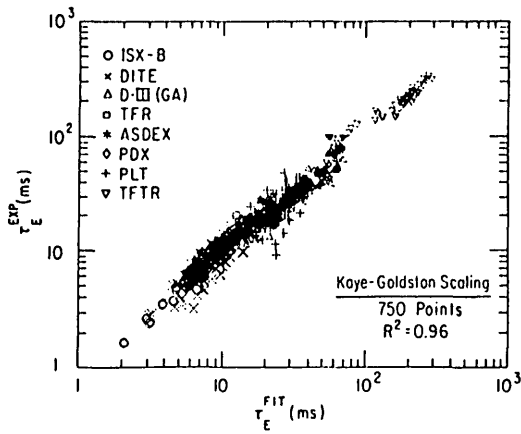


FIG. 6. Total energy confinement time plotted against the empirical Kaye-Goldston scaling for L-mode data from NBI heated experiments.

$$\tau_E(0) \propto \left(\frac{P_T}{n_0}\right)^{0.4} B_T^{0.8} \quad (54)$$

In the absence of published empirical scalings for $T_i(0)$, it is clear that if it can be assumed that $T_i(0) \propto T_e(0)$, then Eq. (52) also correlates with the observations. With regard to the confinement time, Eq. (53) is in reasonable agreement with most of the parametric dependences exhibited by the Kaye-Goldston formula [2]

$$\tau_E \propto n_0^{0.3} P_T^{-0.6} R^{1.7} I_p^{1.2} a^{-0.5} B_T^{-0.1} \quad (55)$$

This empirical result comes from a statistical regression analysis of a large database for NBI heated L-mode discharges. The experimental values for τ_E from numerous tokamaks are plotted against Eq. (55) in Fig. 6.

5. CONCLUSIONS

The basic proposition presented in this paper is that profile-consistent microinstability-based models for anomalous thermal transport can produce reasonable correlation with most of the significant confinement properties observed in tokamak experiments. In particular, invoking the presence of trapped-electron drift modes (for $\eta_i \leq (\eta_i)_c$) and toroidal ion temperature gradient modes (for $\eta_i > (\eta_i)_c$) in the good confinement region (between the $q = 1$ and $q = 2$ surfaces) leads to predicted scalings for τ_E ,

$T_e(0)$ and $\langle T_e \rangle$, in good agreement with experimental results. As demonstrated in Section 3, application of the profile constraint formulated in Section 2 ensures consistency with the experimentally deduced profiles for $\chi_e(r)$ and $T_e(r)$. The profile constraint also accounts for the favourable dependence of $\chi_j(r)$ on the current. In Ohmic discharges this trend is obscured by the fact that $\chi_j(r)$ has an adverse dependence on the heating power (see, for instance, Eq. (36)) which increases with current. On the other hand, in NBI heated discharges the beam power, which is independent of current, is usually much greater than P_Ω so that the favourable scaling with I_p is more evident.

In addition to the Ohmic and NBI heated L-mode classes of discharges investigated, it is also of considerable interest to further develop the profile-consistent microinstability transport models for application to H-mode cases, to wave-heated plasmas (ECH, ICRF, etc.), to pellet injection refuelling experiments, and to ignition scenarios. This will involve properly specifying steady state deposition profiles and accounting for possible electromagnetic effects (e.g. kinetic ballooning modes and finite-beta modified electrostatic instabilities [6, 42]) in higher beta plasmas. For the higher beta conditions and especially for shaped cross-section applications, the simple cylindrical form of the steady state energy balance equations used here should be appropriately generalized. With regard to proposed ignition experiments, recent zero-dimensional scaling studies have indicated that the presence of trapped-electron drift modes [43] and η_i -type instabilities [44] can dramatically influence the density limit in such systems. Hence, profile-consistent models, which account for alpha-particle heating and radiation losses together with the microinstability effects, need to be developed for use in transport code studies of likely ignition scenarios.

As discussed in Section 4, the parameter $\eta_i \equiv d \ln T_i / d \ln n_0$ is the primary indicator of the extent to which the ion channel is dominated by anomalous losses. The exact threshold value is difficult to calculate [32] and is usually estimated to fall in the range $(\eta_i)_c \sim 1$ to 2. It is interesting to note that recent steady state transport code studies have indicated that the computed ion temperature profiles (in the presence of toroidal η_i -modes) tend to adjust themselves to values of η_i near $(\eta_i)_c$ [40]. Of course, this parameter is also strongly dependent on the dynamics governing the density profile. Unfortunately, no compelling physics-based model has as yet been established to simulate realistically the observed

particle transport properties. Hence, in the present study as well as in other recent confinement studies [30, 31, 39, 40, 43], the steady state density profile is simply assumed to have the empirical parabolic shape, $n(r) = n_0[1 - (r/a)^2]^{\alpha n}$.

As a final point it should be emphasized that even if the profile-consistent microinstability type models presented in this paper continue to be reasonably successful in predicting experimentally observed thermal confinement trends, they still leave a number of important physics questions unanswered. Foremost among these is a first principles justification of the empirical profile consistency constraint used in these models. In other words, a theory is needed to explain how this constraint is indeed enforced across the discharge. This would require the identification of the dominant mechanisms responsible for the large transport effects in the $q > 2$ region of the plasma. Since tearing mode activity can lead to the destruction of good magnetic surfaces [17], it appears to be an attractive candidate. However, in the case of lower current discharges with associated large values of q_a , it does not appear that such strong effects could be excited [40]. Since the level of confidence in the predictive capability of any theoretical model rests on the degree to which it is justified by first principles physics, the theoretical resolution of this profile consistency problem needs to be vigorously pursued.

ACKNOWLEDGEMENTS

The author gratefully acknowledges many stimulating discussions with B. Coppi on the subject of profile consistency, with F.W. Perkins and R. Waltz about general scaling trends, and with G. Rewoldt about the key properties of toroidal microinstabilities. Special thanks are also extended to S. Kaye, R. Goldston, G. Taylor, P. Efthimion and K. McGuire for both providing and explaining key features of the experimental database used in these studies.

This work was supported by the United States Department of Energy under Contract No. DE-AC02-76-CHO-3073.

REFERENCES

- [1] GOLDSTON, R.J., *Plasma Phys. Controll. Fusion* 26 (1984) 87.
- [2] KAYE, S.M., *Phys. Fluids* 28 (1985) 2327.
- [3] GROEBNER, R.J., PFEIFFER, W.W., BLAU, F.P., BURRELL, K.H., FAIRBANKS, E.S., SERAYDARIAN, R.P., *Nucl. Fusion* 26 (1986) 543.
- [4] TANG, W.M., *Nucl. Fusion* 18 (1978) 1089.
- [5] LIEWER, P.C., *Nucl. Fusion* 25 (1985) 543.
- [6] REWOLDT, G., TANG, W.M., FRIEMAN, E.A., *Phys. Fluids* 21 (1978) 1531; REWOLDT, G., TANG, W.M., CHANCE, M.S., *Phys. Fluids* 25 (1982) 480.
- [7] PFEIFFER, W., WALTZ, R.E., *Nucl. Fusion* 19 (1979) 51.
- [8] TAYLOR, G., EFTHIMION, P.C., ARUNASALAM, V., GOLDSTON, R.J., GREK, B., et al., *Nucl. Fusion* 26 (1986) 339.
- [9] COPPI, B., *Comm. Plasma Phys. Controll. Fusion* 5 (1980) 261.
- [10] FAIRFAX, S., GONDHALEKAR, A., GRANETZ, R., GREENWALD, M., GWINN, D., et al., in *Plasma Physics and Controlled Nuclear Fusion Research 1980 (Proc. 8th Int. Conf. Brussels, 1980)*, Vol. 1, IAEA, Vienna (1981) 439.
- [11] MURAKAMI, M., and TFTR GROUP, in *Controlled Fusion and Plasma Physics (Proc. 12th Europ. Conf. Budapest, 1985)*, European Physical Society (1985).
- [12] GREENWALD, M., and ALCATOR GROUP, *Phys. Rev. Lett.* 53 (1984) 352.
- [13] HINTON, F.L., HAZELTINE, R.D., *Rev. Mod. Phys.* 48 (1976) 239.
- [14] MIRNOV, S.V., in *Plasma Physics and Controlled Nuclear Fusion Research 1978 (Proc. 7th Int. Conf. Innsbruck, 1978)*, Vol. 1, IAEA, Vienna (1979) 433.
- [15] EQUIPE TFR, *Nucl. Fusion* 20 (1980) 1227.
- [16] RAZUMOVA, K.A., *Plasma Phys. Controll. Fusion* 26 (1984) 37.
- [17] WHITE, R.B., GOLDSTON, R.J., MCGUIRE, K., BOOZER, A.H., MONTICELLO, D.A., PARK, W., *Phys. Fluids* 26 (1983) 2958.
- [18] DUPREE, T.H., *Phys. Fluids* 10 (1967) 1049.
- [19] CHENG, C.Z., CHEN, L., *Nucl. Fusion* 21 (1981) 403.
- [20] ADAM, J.C., TANG, W.M., RUTHERFORD, P.H., *Phys. Fluids* 19 (1976) 561.
- [21] DOBROWOLNY, M., NOCENTINI, A., *Plasma Phys.* 16 (1974) 433.
- [22] TANG, W.M., REWOLDT, G., CHEN, L., *Microinstabilities in Weak Density Gradient Tokamak Systems*, Princeton Plasma Physics Lab. Rep. PPPL-2337 (1986); *Phys. Fluids* 29 11 (1986).
- [23] BRAGINSKII, S.I., in *Reviews of Plasma Physics* (LEONTOVICH, M.A., Ed.), Vol. 1, Consultants Bureau, New York (1965) 205.
- [24] KAYE, S.M., GOLDSTON, R.J., BELL, M., BOL, K., BITTER, M., et al., *Nucl. Fusion* 24 (1984) 1303.
- [25] KAYE, S.M., private communication, 1985.
- [26] TOWNER, H.H., EFTHIMION, P.C., ZARNSTORFF, M.C., *Bull. Am. Phys. Soc.* 30 (1985) 1518.
- [27] PFEIFFER, W., WALTZ, R.E., *Nucl. Fusion* 19 (1979) 51.
- [28] EFTHIMION, P.C., BRETZ, N., BELL, M., BITTER, M., BLANCHARD, W.R., et al., in *Plasma Physics and Controlled Nuclear Fusion Research 1984 (Proc. 10th Int. Conf. London, 1984)*, Vol. 1, IAEA, Vienna (1985) 29.
- [29] REDDI, M., private communication, 1985.

- [30] PERKINS, F.W., in Heating in Toroidal Plasmas (Proc. 4th Int. Symp. Rome, 1984), Vol. 2, Int. School of Plasma Physics, Varenna (1984) 977.
- [31] TANG, W.M., CHENG, C.Z., KROMMES, J.A., LEE, W.W., OBERMAN, C.R., et al., in Plasma Physics and Controlled Nuclear Fusion Research 1984 (Proc. 10th Int. Conf. London, 1984), Vol. 2, IAEA, Vienna (1985) 213.
- [32] GUZDAR, P.N., CHEN, L., TANG, W.M., RUTHERFORD, P.H., Phys. Fluids **26** (1983) 673.
- [33] MANHEIMER, W.M., OTT, E., TANG, W.M., Phys. Fluids **20** (1977) 806.
- [34] WALTZ, R.E., GUEST, G.E., Phys. Rev. Lett. **42** (1979) 651.
- [35] LIEWER, P.C., PFEIFFER, W., WALTZ, R.E., Phys. Fluids **26** (1983) 563.
- [36] EJIMA, S., PETRIE, T.W., RIVIERE, A.C., ANGEL, T.R., ARMENTROUT, C.J., et al., Nucl. Fusion **22** (1982) 1627.
- [37] BLACKWELL, B., FIORE, C.L., GANDY, R., GONDHALEKAR, A., GRANETZ, R.S., et al., in Plasma Physics and Controlled Nuclear Fusion Research 1982 (Proc. 9th Int. Conf. Baltimore, 1982) Vol. 2, IAEA Vienna (1983) 27.
- [38] COPPI, B., Sherwood Annual Controlled Fusion Theory Conference (Proc. Mtg Incline Village, NV, 1984), (1984) Paper 3A3.
- [39] DOMINGUEZ, R.R., WALTZ, R.E., Tokamak Transport Code Simulations with Drift Wave Models, GA Technologies Inc., San Diego, CA, Rep. GA-18184 (1986).
- [40] ROMANELLI, F., TANG, W.M., WHITE, R.B., Nucl. Fusion **26** (1986) 1515.
- [41] TANG, W.M., ADAM, J.C., ROSS, D.W., Phys. Fluids **20** (1977) 430.
- [42] TANG, W.M., REWOLDT, G., CHENG, C.Z., CHANCE, M.S., Nucl. Fusion **25** (1985) 151.
- [43] PERKINS, F.W., SUN, Y.C., On Confinement Scaling and Ignition in Tokamaks, Princeton Plasma Physics Lab. Rep. PPPL-2261 (1985).
- [44] COPPI, B., TANG, W.M., Influence of Anomalous Thermal Losses on Ignition Conditions, Princeton Plasma Physics Lab. Rep. PPPL-2343 (1986).

(Manuscript received 27 January 1986

Final manuscript received 25 July 1986)